Carcinogenesis vol.35 no.4 pp.849–858, 2014
doi:10.1093/carcin/bgt377
Advance Access publication November 26, 2013

LGR5 positivity defines stem-like cells in colorectal cancer

Daniela Hirsch[1,2], Nick Barker[3], Nicole McNeil[1], Yue Hu[1], Jordi Camps[1], Katherine McKinnon[4], Hans Clevers[5], Thomas Ried[1,*] and Timo Gaiser[6]

[1]Section of Cancer Genomics, Genetics Branch, Center for Cancer Research, National Cancer Institute, National Institutes of Health, Bethesda, MD 20892, USA, [2]Experimental Medicine and Therapy Research, University of Regensburg, 93053 Regensburg, Germany, [3]Institute of Medical Biology, Singapore 138648, Singapore, [4]FACS Core Facility, Vaccine Branch, Center for Cancer Research, National Cancer Institute, National Institutes of Health, Bethesda, MD 20892, USA, [5]Hubrecht Institute, 3584 CT Utrecht, The Netherlands and [6]Institute of Pathology, University Medical Center Mannheim, 68167 Mannheim, Germany

*To whom correspondence should be addressed. Tel: +1 301 5943118; Fax: +1 301 4021204;
Email: riedt@mail.nih.gov

Correspondence may also be addressed to Timo Gaiser. Tel: +49 621 3832556; Fax: +49 621 3832005;
Email: timo.gaiser@umm.de

Like normal colorectal epithelium, colorectal carcinomas (CRCs) are organized hierarchically and include populations of cells with stem-like properties. Leucine-rich-repeat-containing G-protein-coupled receptor 5 (LGR5) is associated with these stem cells in normal colorectal epithelium; however, the precise function of LGR5 in CRC remains largely unknown. Here, we analyzed the functional and molecular consequences of short hairpin RNA-mediated silencing of *LGR5* in CRC cell lines SW480 and HT-29. Additionally, we exposed *Lgr5-EGFP-IRES-CreERT2* mice to azoxymethane/dextrane sodium sulfate (AOM/DSS), which induces inflammation-driven colon tumors. Tumors were then flow-sorted into fractions of epithelial cells that expressed high or low levels of Lgr5 and were molecularly characterized using gene expression profiling and array comparative genomic hybridization. Silencing of *LGR5* in SW480 CRC cells resulted in a depletion of spheres but did not affect adherently growing cells. Spheres expressed higher levels of several stem cell-associated genes than adherent cells, including *LGR5*. Silencing of *LGR5* reduced proliferation, migration and colony formation *in vitro* and tumorigenicity *in vivo*. In accordance with these results, NOTCH signaling was downregulated upon *LGR5* silencing. In AOM/DSS-induced colon tumors, Lgr5 high cells showed higher levels of several stem cell-associated genes and higher Wnt signaling than Lgr5 low tumor cells and Lgr5 high normal colon cells. Array comparative genomic hybridization revealed no genomic imbalances in either tumor cell fraction. Our data elucidate mechanisms that define the role of LGR5 as a marker for stem-like cells in CRC.

Introduction

Colorectal tumorigenesis is associated with the accumulation of a number of specific genetic changes, which drive the transition from normal epithelium through adenomas to invasive carcinomas. These genetic changes include mutations of specific genes, such as adenomatous polyposis coli (*APC*) and *KRAS*, and tumor-specific genomic imbalances (1–3). Similar to normal colorectal epithelium, colorectal tumors consist of heterogeneous cell populations at various levels of differentiation. Although a few years ago all cells within a tumor were considered to be tumorigenic, recent findings suggested that only a subpopulation of tumor cells can regenerate the tumor (4,5). These cells, termed cancer stem cells (CSCs), may also be involved in therapy resistance, tumor relapse and metastasis. Accordingly, the identification and characterization of these cells was the subject of considerable research efforts. With respect to colorectal carcinomas (CRCs), putative CSCs can be identified by leucine-rich-repeat-containing G-protein-coupled receptor 5 (*Lgr5*; also known as G-protein-coupled receptor 49, *Gpr49*). *Lgr5*, a Wnt target gene that acts as receptor for the Wnt agonist R-spondin, is a marker gene for adult intestinal stem cells as revealed by *in vivo* lineage tracing (6–8). Selective deletion of *Apc* in the mouse in either Lgr5 positive intestinal stem cells or more differentiated cells revealed that mainly the Lgr5 positive stem cell fraction is capable of forming tumors upon Wnt pathway activation, suggesting Lgr5 positive stem cells as the cells-of-origin of intestinal epithelial tumors (9). Although the cell-of-origin for tumorigenesis and the CSC, which propagates the tumor, need not necessarily be identical, *in vivo* lineage tracing provides direct evidence for a stem cell activity of Lgr5 positive cells in mouse intestinal adenomas generated by deletion of *Apc* in Lgr5 positive stem cells (10,11). Resembling the situation in normal intestinal epithelium, adenomas contain a small fraction of Lgr5 positive cells (5–10%) that are able to generate all cell types present within the adenomas, including additional Lgr5 positive cells (11). In human CRC, *LGR5* expression is highly enriched in EPHB2 positive cells, which have similar expression profiles to normal intestinal stem cells and—in contrast to EPHB2 negative cells—display reproducible tumorigenic capacity in immunodeficient mice (12). Cataloging the genetic idiosyncrasies of LGR5 positive and negative cells might help to identify the mechanisms that cause these differences in tumorigenic potential. We have therefore investigated the functional and molecular consequences of short hairpin RNA (shRNA)-mediated *LGR5* silencing in CRC cell lines SW480 and HT-29. To date, studies on LGR5 in primary CRC samples have been constrained by the lack of a reliable antibody against LGR5. We therefore induced inflammation-driven colon tumors in mice that were engineered to contain one enhanced green fluorescent protein (*EGFP*)-tagged *Lgr5* allele (6). This allowed flow cytometric separation of Lgr5 high and low cells based on GFP expression and thus enabled a genome and transcriptome characterization of these two cell fractions. Our loss-of-function experiments conclusively indicate that LGR5 acts as a marker for stem-like cells in CRC.

Abbreviations: AOM, azoxymethane; APC, adenomatous polyposis coli; CRC, colorectal carcinoma; CSC, cancer stem cell; DSS, dextrane sodium sulfate; EGFP, enhanced green fluorescent protein; LGR5, leucine-rich-repeat-containing G-protein-coupled receptor 5; mRNA, messenger RNA; qRT–PCR, quantitative reverse transcription–polymerase chain reaction; shRNA, short hairpin RNA.

Materials and methods

Cell lines and lentiviral transduction

The six human CRC cell lines (Caco-2, HCT 116, HT-29, SW480, SW620 and T84) were purchased from the American Type Culture Collection (Manassas, VA). All cell lines were cultured in media as recommended by the American Type Culture Collection supplemented with fetal bovine serum (10% v/v), L-glutamine (2 mM), penicillin (100 U/ml) and streptomycin (100 µg/ml). Lentiviral shRNA transduction of SW480 and HT-29 cells was done using high-titer lentivirus (Clone ID: V3LHS_635055, Open Biosystems, Thermo Fisher Scientific, Lafayette, CO) according to the manufacturer's instructions.

Mice

Athymic nude mice (strain NCr-nu/nu) were obtained from Frederick National Laboratory for Cancer Research (Frederick, MD). Heterozygous *Lgr5-EGFP-IRES-CreERT2* mice [strain B6.129P2-Lgr5tm1(cre/ERT2)Cle/J, henceforth referred to as *'Lgr5-EGFP mice'*] were ordered from Jackson Laboratory (Bar Harbor, ME) (6). All mice were bred and housed in a pathogen-free environment and used in experiments in accordance with institutional guidelines at the Center for Cancer Research, National Cancer Institute, National Institutes of Health. All experimental procedures conducted in this study were approved by the Animal Care and Use Committee of the National Institutes of Health.

Tumorigenicity assay

Tumorigenicity assay was performed as described previously (13).

Microarray gene expression profiling of cell lines

Total RNA was isolated from SW480 sh*LGR5* and control cells and from SW480 spheres and adherent cells using the RNeasy Mini Kit (Qiagen, Hilden, Germany) including DNase I treatment (RNase-Free DNase Set, Qiagen). RNA integrity was assessed by 2100 Bioanalyzer (RNA 6000 Nano LabChip Kit, Agilent Technologies, Santa Clara, CA). Appropriate *LGR5* status was confirmed by real-time quantitative reverse transcription–polymerase chain reaction (qRT–PCR). Total RNA (700 ng) was labeled using the Quick Amp Labeling Kit, one-color (Agilent) and subsequently hybridized on Human GE 4x44K v2 Microarrays (Agilent) according to the manufacturer's protocol version 6.5. Slides were scanned with microarray scanner G2565BA (Agilent). Images were analyzed and data were quality controlled using Feature Extraction software version 10.7.1.1 (Agilent).

Carcinogen-induced inflammation-driven colon tumorigenesis model

To induce colon tumors, *Lgr5-EGFP* mice aged 2–4 months were injected with azoxymethane (AOM, 12.5 µg/g body weight; A5486, Sigma, St Louis, MO) twice and subjected to three cycles of dextrane sodium sulfate (DSS, 2.5%; molecular weight = 36 000–50 000, MP Biomedicals, Solon, OH) in the drinking water (14,15). Tumor growth was monitored by colonoscopies. About 100 days after the first AOM injection, mice were killed.

RNA amplification and microarray gene expression profiling of flow-sorted normal mouse colons and mouse colon tumors

RNA isolated from flow-sorted normal mouse colons and mouse colon tumors was amplified together with spike-ins (1 µl of a 1:50 000 dilution per reaction, One-Color RNA Spike-In Kit, Agilent) using the Ovation Pico WTA System (NuGEN Technologies, San Carlos, CA). The amplified complementary DNA was labeled using the BioPrime® Total Genomic Labeling Module (Invitrogen, Life Technologies, Carlsbad, CA) and subsequently 4 µg of Alexa Fluor® 3 labeled target was hybridized on Whole Mouse Genome Microarrays 4x44K (Agilent) according to NuGEN's Agilent Solution Application Note #1. Scanning, image analysis and data quality control were done as for cell lines.

DNA amplification and array comparative genomic hybridization of flow-sorted mouse colon tumors

DNA amplification and array comparative genomic hybridization were performed as described previously and are summarized in Supplementary Materials and methods, available at *Carcinogenesis* Online (16). Array-based comparative genomic hybridization data have been deposited in Gene Expression Omnibus database (data accession number: GSE46711).

Statistical analysis

Differences between groups were estimated by Student's *t*-test, Fisher's exact test or two-way repeated measures analysis of variance (one factor repetition). $P < 0.05$ was considered significant.

Microarray gene expression analysis

Log2 intensities were normalized to the 75% percentile according to the manufacturer's protocol (Agilent). Only probes with intensities higher than 50 were used for the analysis. Unsupervised hierarchical clustering with Euclidean distance and Ward method was performed with Genomics Suite™ software (Partek Incorporated, St Louis, MO). The corresponding functional annotation of differentially expressed genes and their affiliation with specific genetic pathways were interrogated using Ingenuity Pathway Analysis software (Ingenuity Systems, Redwood City, CA). Microarray gene expression data have been deposited in Gene Expression Omnibus database (data accession number: GSE46200).

Results

LGR5 is overexpressed in human CRC cell lines

LGR5 expression is upregulated in primary CRC samples compared with normal colorectal epithelium (17). Using real-time qRT–PCR, we could show that *LGR5* expression was also upregulated in CRC cell lines Caco-2, HT-29, SW480, SW620 and T84 (Figure 1A) (18,19). The only cell line without overexpression of *LGR5* was HCT 116. This is consistent with recent findings, suggesting that HCT 116 may not be organized hierarchically and may therefore not contain a stem-like cell fraction (13,20,21).

LGR5 silencing leads to depletion of a morphologically distinct subpopulation of SW480 CRC cells

To investigate the function of *LGR5* in CRC, we transduced two CRC cell lines (SW480 and HT-29), which both showed a similar moderate overexpression of *LGR5*, with lentiviral shRNA constructs. This significantly reduced *LGR5* expression compared with empty vector control (henceforth referred to as 'control') cells as assessed by real-time qRT–PCR (Figure 1B). In SW480, silencing of *LGR5* led to a remarkable morphologic change, whereas HT-29 did not display an apparent difference (Figure 1C). Unlike HT-29, SW480 typically comprises two morphologically distinct subpopulations, i.e. spheres and adherent cells, when cultured in serum-containing medium. Upon *LGR5* silencing, spheres were completely depleted and only an adherent cell layer remained. Spheres, along with *LGR5* expression, remained undetectable in SW480 sh*LGR5* cells over more than 12 months of continuous passage, demonstrating long-lasting effects of the shRNA on *LGR5* expression. To exclude that the disappearance of spheres was induced by cell splitting, we next separately analyzed *LGR5* messenger RNA (mRNA) expression in spheres and adherent cells of SW480 control cells. Although *LGR5* was highly expressed in spheres, adherent cells displayed virtually no *LGR5* expression, supporting our conclusion that the morphologic change was caused by silencing of *LGR5* (Figure 1D).

LGR5 silencing in SW480 and HT-29 CRC cells reduces proliferation, migration and colony formation in vitro

To evaluate the influence of *LGR5* on cell proliferation, we compared the cleavage of the tetrazolium salt WST-1 between sh*LGR5* and control cells. Upon silencing of *LGR5*, cleavage of WST-1 was significantly decreased in HT-29 cells (Figure 2A). SW480 cells showed the same tendency although not reaching statistical significance ($P = 0.096$). This might be attributable to the loss of spheres in SW480 upon silencing of *LGR5*; spheres usually grow slower than isogenic adherent cells (22). In other words, the proliferating cells of SW480 reside within the *LGR5* low adherent cells and not within the *LGR5* high spheres. This explains the small effect of *LGR5* silencing on proliferation in SW480.

The effect of *LGR5* on migration was assessed by wound healing and transwell migration assays. In the wound healing assay, SW480 sh*LGR5* cells tended to cover a smaller area of the initial scratch than respective control cells at all time points, reaching statistical significance after 72 h (Figure 2B). To reduce the impact of proliferation as a confounding variable, we additionally monitored migration for each group through transwell membranes and observed a significantly smaller number of migrated sh*LGR5* cells compared with control cells after incubating for 24 h (Figure 2C). For HT-29, none of the assays allowed a proper assessment of migration dependent on *LGR5* status owing to too little migratory activity of HT-29 cells in our experiments.

In the colony formation assay, both cell lines formed significantly fewer colonies when *LGR5* was silenced compared with control cells (Figure 2D).

LGR5 silencing reduces tumorigenic capacity of SW480 CRC cells after xenotransplantation

To corroborate our *in vitro* colony formation results *in vivo*, we injected CRC cells with differential *LGR5* expression levels subcutaneously into the flanks of nude mice and followed the appearance of tumors. SW480 sh*LGR5* cells were less tumorigenic than control cells and the tumors grew slower (Table I and Supplementary Figure S1A–C, available at *Carcinogenesis* Online). Reduced tumorigenicity was not observed for HT-29 cells upon *LGR5* silencing (Table I). However, tumors derived from HT-29 sh*LGR5* cells also grew slower than those from control cells (Supplementary Figure S1D, available at *Carcinogenesis* Online). Sufficient silencing of *LGR5* in xenografts was confirmed by real-time qRT–PCR (Supplementary Figure S1E, available at *Carcinogenesis* Online).

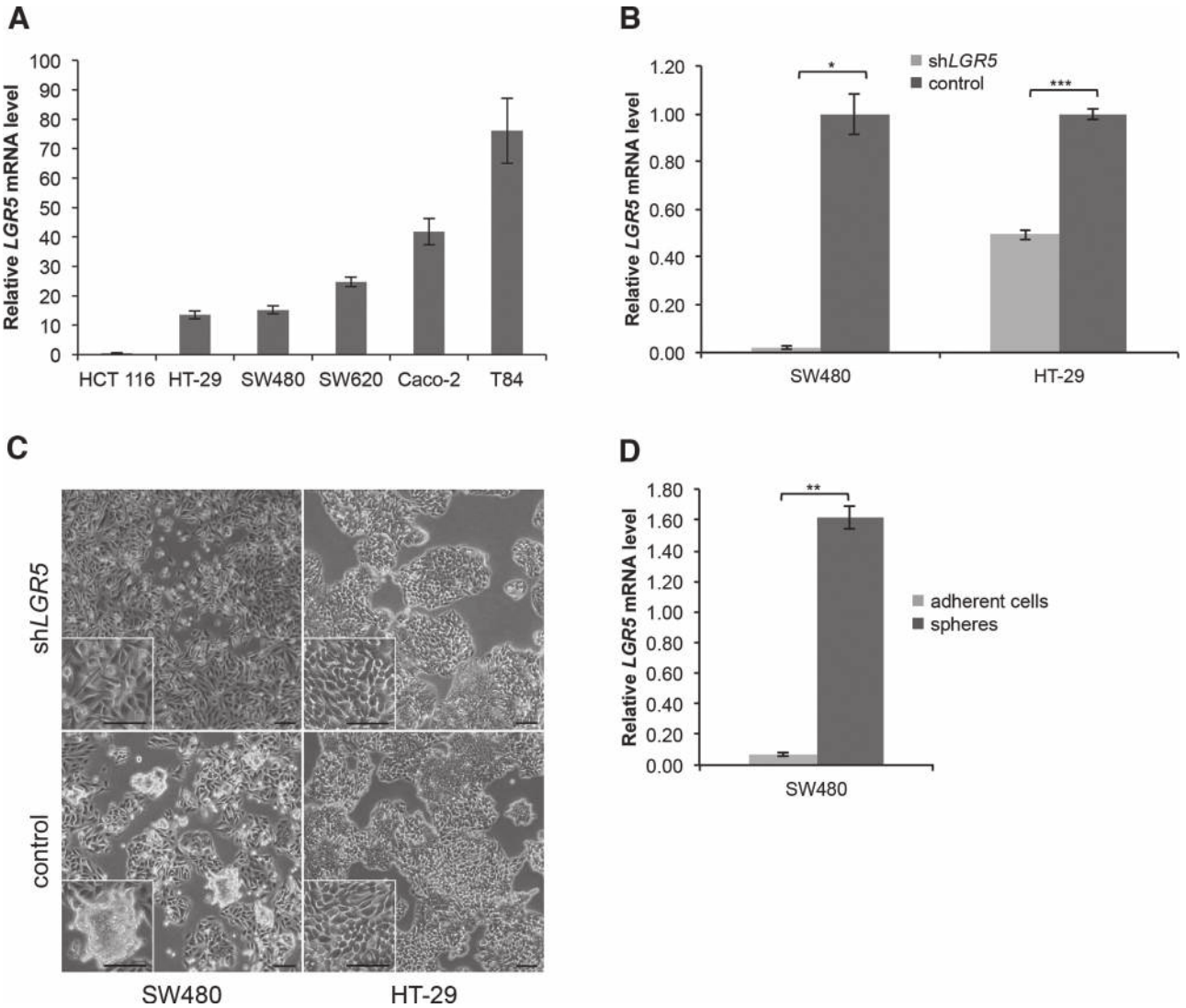

Fig. 1. Expression levels of *LGR5* in CRC cell lines and shRNA-mediated silencing of *LGR5* in SW480 and HT-29 CRC cells. (**A**) *LGR5* mRNA levels in CRC cell lines as determined by real-time qRT–PCR. *LGR5* mRNA levels were normalized to *YWHAZ* and are expressed as fold changes relative to normal colorectal epithelial cells. Columns and error bars represent means ± SEM of two independent experiments using triplicate measurements in each experiment. (**B**) *LGR5* silencing efficiency in CRC cell lines SW480 and HT-29 upon lentiviral shRNA transduction as determined by real-time qRT–PCR. *LGR5* mRNA levels were normalized to *YWHAZ* and are expressed as fold changes relative to control. Columns and error bars represent means ± SEM of three independent experiments using triplicate measurements in each experiment. (**C**) Representative phase-contrast images of SW480 and HT-29 cells upon *LGR5* silencing. SW480 is composed of two morphologically distinct subpopulations (spheres and adherent cells), whereas HT-29 shows one phenotype. After *LGR5* silencing, spheres in SW480 were completely lost with no apparent changes in HT-29. Scale bars, 100 µm. (**D**) Expression of *LGR5* in spheres versus adherent cells of SW480. Spheres express high levels of *LGR5*, whereas in adherent cells, virtually no *LGR5* expression can be detected by real-time qRT–PCR. *LGR5* mRNA levels were normalized to *YWHAZ* and are expressed as fold changes relative to control. Data represent means ± SEM of three independent experiments using triplicate measurements in each experiment. $*P < 0.05$, $**P < 0.005$ and $***P < 0.0005$.

Lacking a reliable LGR5 antibody, we utilized the phenotypic change of SW480 upon *LGR5* silencing to separate *LGR5* high cells (spheres) and *LGR5* low cells (adherent cells), which we then injected subcutaneously into the flanks of nude mice as a proof-of-principle experiment. Confirming our hypothesis, only *LGR5* high cells generated tumors; however, the small number of animals prevented reaching statistical significance ($P = 0.40$) (Table I).

NOTCH signaling is downregulated upon LGR5 silencing

To examine whether differential *LGR5* expression levels in CRC cells would be reflected in specific changes to the cellular transcriptome, we performed microarray gene expression profiling of SW480 sh*LGR5* and control cells and of SW480 spheres and adherent cells. As *LGR5* silencing in SW480 resulted in a profound morphologic change, we reasoned that genes regulated by *LGR5* might overlap with genes differentially expressed between spheres and adherent cells. Indeed, gene expression profiling revealed a significant overlap of deregulated genes (false discovery rate < 1.0E-103; Figure 3A). These genes included known oncogenes (e.g. *MYB*, *MYCN*) and certain drug efflux genes (e.g. *ABCB1*, *ABCC2*), whose expression was positively correlated with *LGR5* expression. The expression differences between spheres and adherent cells were more pronounced than between sh*LGR5* and control cells, yet unsupervised hierarchical clustering showed a clear separation of all four cell fractions (Figure 3B). Ingenuity Pathway Analysis revealed that the NOTCH signaling pathway was downregulated when *LGR5* was silenced. Conversely, it was upregulated in *LGR5* high spheres. Apart from *LGR5*, spheres also expressed higher levels of several other stem cell-associated genes including *SOX2*, *ALDH1A1* and *SMOC2* when compared with adherent cells (12,23–25). Our gene expression results were

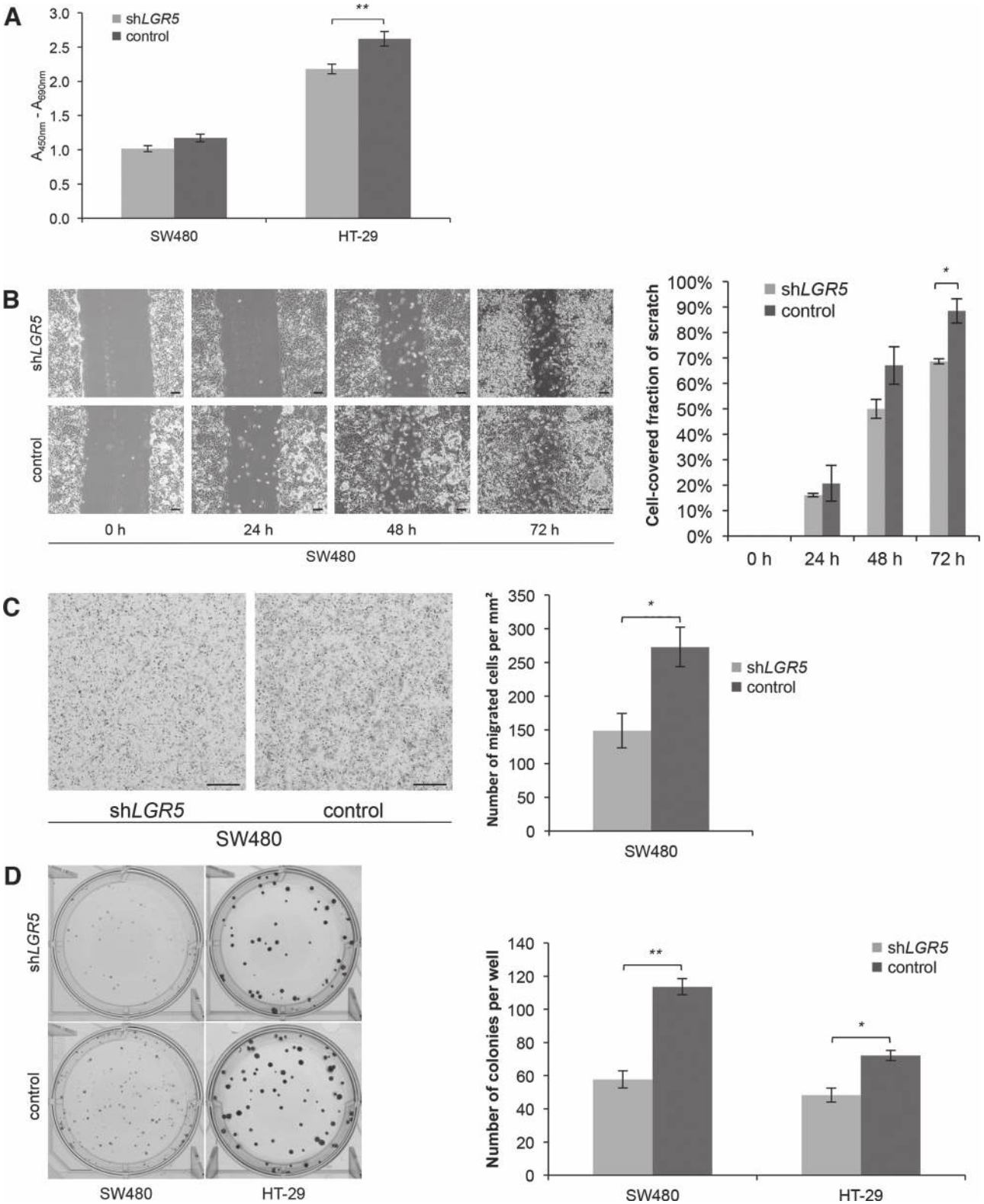

Fig. 2. Functional effects of *LGR5* silencing on SW480 and HT-29 CRC cells. (**A**) *LGR5* silencing decreases proliferation of SW480 and HT-29 CRC cells as quantified based on cleavage of WST-1. Columns and error bars represent means ± SEM of three independent experiments using triplicate measurements in each experiment. (**B**) Silencing of *LGR5* reduces migration in wound healing assays. Columns and error bars represent means ± SEM from one experiment representative of three independent experiments ($n = 6$ scratches per cell type and time point in each experiment). Scale bars, 100 µm. (**C**) In line with the results of the wound healing assay, migration of SW480 sh*LGR5* cells is also decreased in transwell migration assays. Columns and error bars represent means ± SEM from one experiment representative of three independent experiments using triplicate measurements in each experiment. Scale bars, 200 µm. (**D**) *LGR5* silencing substantially reduces colony formation *in vitro*. Each 250 sh*LGR5* and control cells were cultured for 2 weeks. The number of colonies was then assessed using crystal violet staining. Columns and error bars represent means ± SEM of three independent experiments using triplicate measurements in each experiment. $^{*}P < 0.05$ and $^{**}P < 0.005$.

Table I. Quantification of tumor initiation in nude mice after subcutaneous injection of CRC cells with differential levels of *LGR5* expression

Cell line	sh*LGR5* (no. of tumors/no. of injections)	Control (no. of tumors/no. of injections)	No. of injected cells	*P* value
SW480	4/10	9/10	2000	0.0052
	2/5	5/5	20 000	
HT-29	8/10	10/10	2000	0.47
Cell line	Adherent cells (no. of tumors/no. of injections)	Spheres (no. of tumors/no. of injections)	No. of injected cells	*P* value
SW480	0/3	2/3	2000	0.40

exemplarily validated by immunohistochemistry against two differentially expressed genes, cleaved NOTCH1 and SOX6 (Figure 3C).

Lgr5 is overexpressed in AOM/DSS-induced mouse colon tumors but expression is, like in normal colon epithelium, restricted to a small percentage of cells

We next aimed to determine a detailed molecular characterization of Lgr5 positive and negative cells in primary colon tumors. As the lack of a reliable LGR5 antibody prevented these analyses in primary human CRC, we exposed heterozygous *Lgr5-EGFP* mice, harboring one *EGFP*-tagged *Lgr5* allele, to a carcinogen-induced inflammation-driven colon tumorigenesis model based on AOM and DSS (Supplementary Figure S2A, available at *Carcinogenesis* Online) (6,14). All AOM/DSS-induced tumors were restricted to the colon, predominantly located in the rectosigmoid colon, sometimes forming multiple lesions; no lymph node or hematogenous metastases were detectable (Supplementary Figure S2B, available at *Carcinogenesis* Online). Histologically, AOM/DSS-induced colon tumors in *Lgr5-EGFP* mice resembled well-differentiated human tubular adenocarcinomas, mainly of the intramucosal type (Supplementary Figure S2C, available at *Carcinogenesis* Online).

We first examined expression, distribution and frequency of Lgr5 in AOM/DSS-induced colon tumors. Real-time qRT–PCR analysis using RNA isolated from histologically defined tumor and non-tumor regions revealed a significant overexpression of *Lgr5* in AOM/DSS-induced tumors compared with normal colon mucosa (Figure 4A and Supplementary Figure S3A, available at *Carcinogenesis* Online). Immunohistochemistry against GFP showed that, consistent with previous reports, Lgr5-EGFP expressing cells in normal colons were located at the crypt bottoms (Supplementary Figure S3B, available at *Carcinogenesis* Online) (6). In AOM/DSS-induced tumors, Lgr5-EGFP expression was found to be restricted to small populations of scattered cells (Figure 4B). Quantification by flow cytometric analysis revealed that normal colons contained on average 3.8% of Lgr5-EGFP high cells. This percentage was similar to that of AOM/DSS-induced tumors, which harbored on average 3.4% of Lgr5-EGFP high cells (Figure 4C). Supported by the results from our immunohistochemistry-based analysis of Lgr5-EGFP expression, this suggests that a stem cell hierarchy is preserved in AOM/DSS-induced tumors (9,11). However, there were 3 out of 14 (21.4%) AOM/DSS-induced tumors without detectable Lgr5-EGFP expressing cells based on GFP expression, indicating that occasionally also Lgr5-EGFP low cells could acquire the capacity for tumor initiation and/or maintenance (10). This is consistent with observations in human CRC samples, in which LGR5-expressing cells were not detectable in one-third of the analyzed samples, arguing for a frequent stem cell and a rare non-stem cell driven carcinogenesis (12). We confirmed by real-time qRT–PCR that GFP high flow-sorted cells had significantly higher *Lgr5* expression levels than GFP low flow-sorted cells (Figure 4D).

Transcriptome profiles of Lgr5 high and low epithelial cells from AOM/DSS-induced mouse colon tumors are clearly distinct

To examine whether the differential Lgr5 expression levels in normal mouse colons and AOM/DSS-induced mouse colon tumors would be reflected in specific gene expression profiles, we performed microarray gene expression profiling of normal colons and AOM/DSS-induced tumors flow-sorted into Lgr5 high and low fractions based on GFP expression. Reassuringly, the previously described intestinal stem cell-specific genes *Lgr5* and *Smoc2* were upregulated in Lgr5 high normal and tumor cells compared with Lgr5 low normal and tumor cells (12,25). In addition, Lgr5 high tumor cells showed increased expression of *EphB2*, which is known to be coexpressed with Lgr5 (12). Unsupervised hierarchical clustering showed a clear separation between Lgr5 high and low tumor cells; however, separation according to Lgr5 expression levels was not as clear in normal cells (Figure 5A). Ingenuity Pathway Analysis revealed that the Wnt signaling pathway was upregulated in Lgr5 high tumor cells compared with Lgr5 low tumor cells and also with Lgr5 high normal colon epithelial cells. Gene expression results were exemplarily validated by immunohistochemistry against Sox6 (Figure 5B).

Lgr5 high and low epithelial cells from AOM/DSS-induced mouse colon tumors are both chromosomally stable

Genomic imbalances influence gene expression patterns (26). To exclude that the transcriptional differences between Lgr5 high and low tumor cells were imposed by distinct patterns of chromosomal aberrations in the two cell fractions, we additionally performed array comparative genomic hybridization from the flow-sorted AOM/DSS-induced mouse colon tumors. All eight tumors were chromosomally stable, and thus, no difference between Lgr5 high and low cells could be detected (Supplementary Figure S4, available at *Carcinogenesis* Online) (27). This indicates that other mechanisms, for instance epigenetics, may be the driving force in AOM/DSS-induced mouse colon tumors (28). In conclusion, these data conclusively indicate that LGR5 marks stem-like CRC cells and defines a cell compartment in which proliferating, migrating and tumorigenic CRC cells are enriched. This is consistent with the observed upregulation of stem cell-related signaling pathways such as NOTCH or Wnt in LGR5 high CRC cells.

Discussion

Here, we studied the functional and molecular consequences of *LGR5* silencing in CRC cell lines and identified LGR5 as a marker for stem-like cells in CRC. Based on Lgr5 expression, we defined a gene expression signature for stem-like cells in CRC using an inflammation-driven mouse colon tumorigenesis model based on AOM and DSS, which mimics sporadic CRC development.

To understand the role of LGR5 in colorectal tumorigenesis, which is controversial, we silenced its expression in two CRC cell lines (SW480 and HT-29) (18,29–34). Silencing of *LGR5* in these cell lines resulted in reduced proliferation, migration and colony formation *in vitro* as well as reduced tumorigenicity *in vivo*. This is consistent with previous studies targeting *LGR5* in various cancer entities including basal cell carcinoma, gastric cancer, glioblastoma and CRC (18,29,31–34). In these cancers, expression of *LGR5* was associated with increased cell proliferation, migration and invasion and decreased apoptosis. In turn, silencing of *LGR5* in these cancers decreased proliferation, colony formation and tumorigenicity and enhanced apoptosis. Upregulation of *LGR5* in non-tumorigenic NIH3T3 fibroblasts

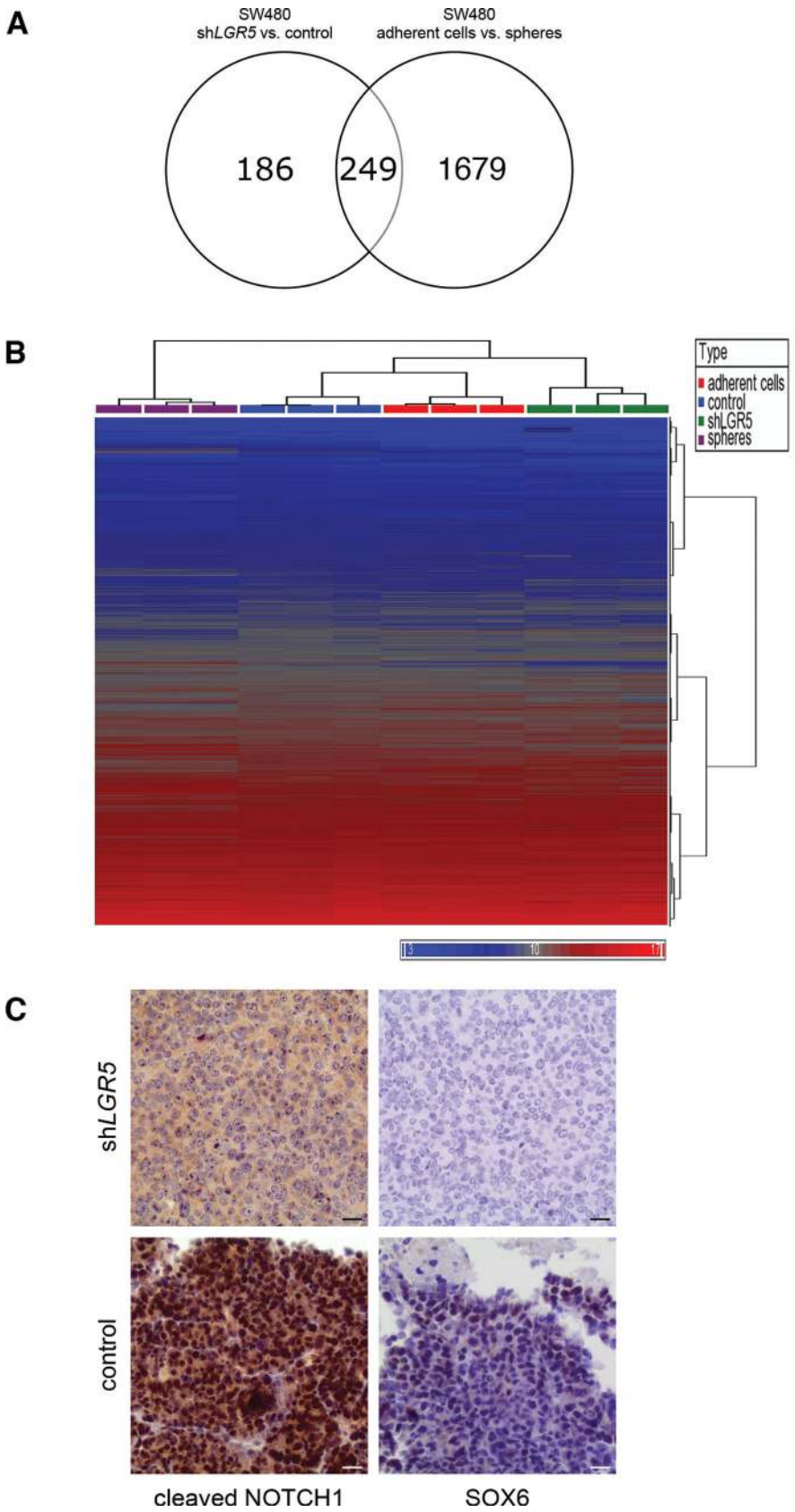

Fig. 3. Gene expression profiling of sh*LGR5* versus control cells and adherent cells versus spheres of SW480. (**A**) Venn diagram showing a significant overlap of differentially expressed genes when comparing sh*LGR5* versus control cells and adherent cells versus spheres of SW480 (false discovery rate < 1.0E-103). (**B**) Unsupervised hierarchical clustering based on gene expression profiles of sh*LGR5* and control cells as well as adherent cells and spheres from SW480. Samples cluster by cell type first. The different *LGR5* fractions are clearly separated. (**C**) In line with our gene expression data, immunohistochemistry against both cleaved NOTCH1 and SOX6 also shows a lower expression in SW480 sh*LGR5* than in SW480 control cell derived xenograft tumors. Scale bars, 20 µm.

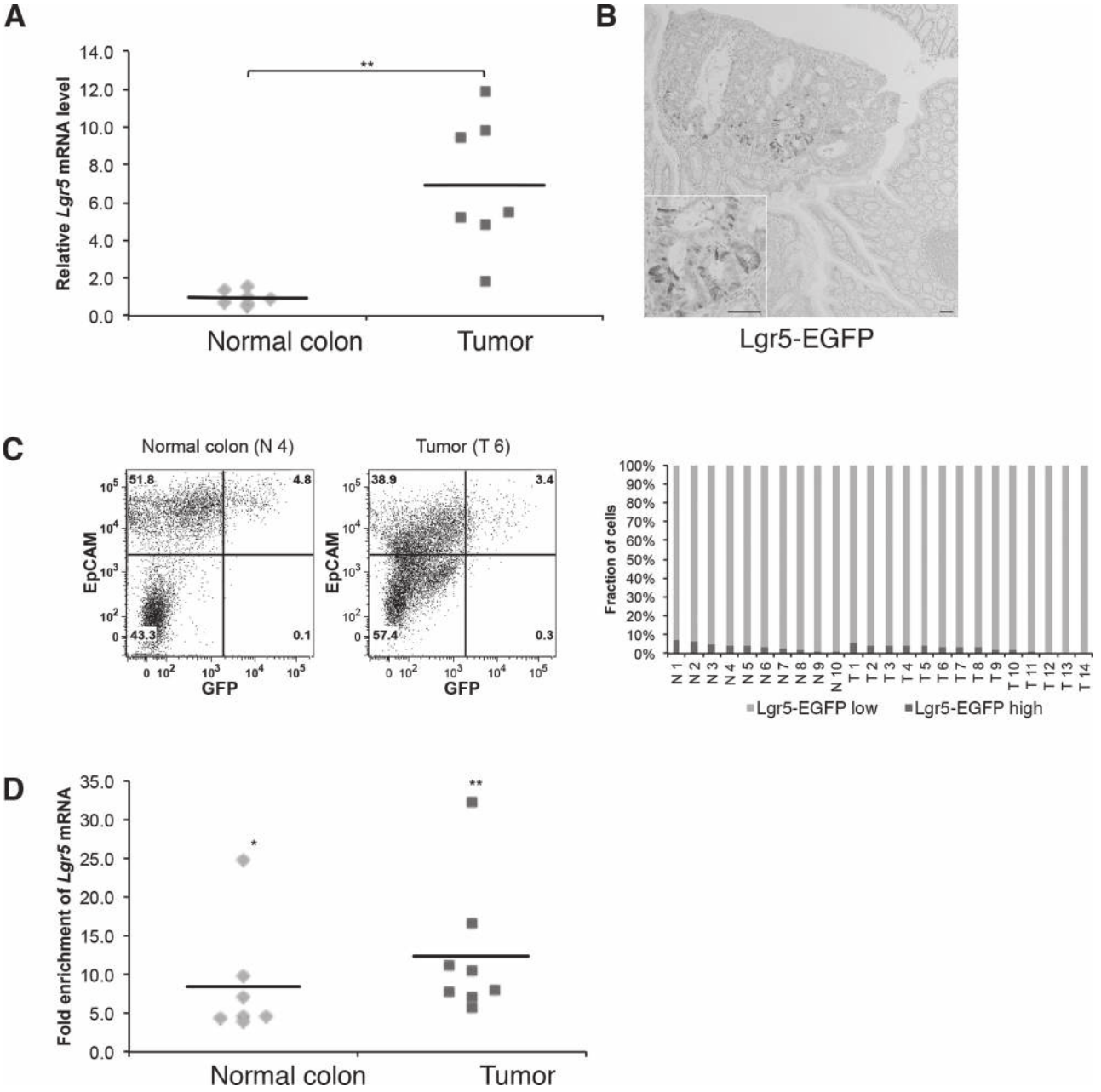

Fig. 4. Expression, distribution and frequency of Lgr5 in AOM/DSS-induced mouse colon tumors. (**A**) Varying degrees of overexpression of *Lgr5* in AOM/DSS-induced colon tumors as determined by real-time qRT–PCR. *Lgr5* mRNA levels were normalized to *Gapdh* and are expressed as fold changes relative to normal adjacent colon. Horizontal lines represent means. Triplicate measurements were used for each data point. (**B**) Lgr5-EGFP expression in AOM/DSS-induced colon tumors is restricted to small populations of scattered cells. Scale bars, 50 µm. (**C**) Quantification of Lgr5-EGFP high cells by flow cytometric analysis revealed that both normal colons and AOM/DSS-induced tumors contain similar small percentages of Lgr5-EGFP high cells. N, normal colon; T, tumor. (**D**) *Lgr5* expression is enriched in flow-sorted Lgr5-EGFP high normal colon or colon tumor cells compared with respective Lgr5-EGFP low normal colon or colon tumor cells as determined by real-time qRT–PCR. *Lgr5* mRNA levels were normalized to *Gapdh*. Horizontal lines represent means. Triplicate measurements were used for each data point. $*P < 0.05$ and $**P < 0.005$.

and in HaCat keratinocytes induced colony formation and promoted tumorigenicity (18,29).

For reasons that remain to be understood, all those results are in contrast to the findings by Walker and colleagues in CRC cell lines LIM1215 and LIM1899. Upon silencing of *LGR5*, they reported increased migration, colony formation and tumorigenicity, and opposite phenotypes when *LGR5* was overexpressed (30).

The reduced tumorigenic capacity of SW480 *in vivo* upon *LGR5* silencing, along with the decreased colony formation *in vitro*, suggests that LGR5 expression is associated with stem-like properties in this cell line. The observation that sh*LGR5* and control HT-29 cells were equally tumorigenic upon xenotransplantation is somewhat contradictory but might be either explained by the lower silencing efficiency or because tumorigenicity of HT-29 does not depend on LGR5 expression. Also, HT-29 has much lower Wnt activity (35). The number of injected cells might have been too high to reveal differences since HT-29 is a highly tumorigenic cell line. Alternatively, the reduction of tumor growth rate but not tumor incidence upon *LGR5* silencing in HT-29 might suggest that *LGR5* silencing affects tumor propagation rather than tumor initiation in this cell line. The slower tumor growth rate upon silencing of *LGR5* for both SW480 and HT-29 cells is consistent with previous data showing that Lgr5 positive cells are actively proliferating (6).

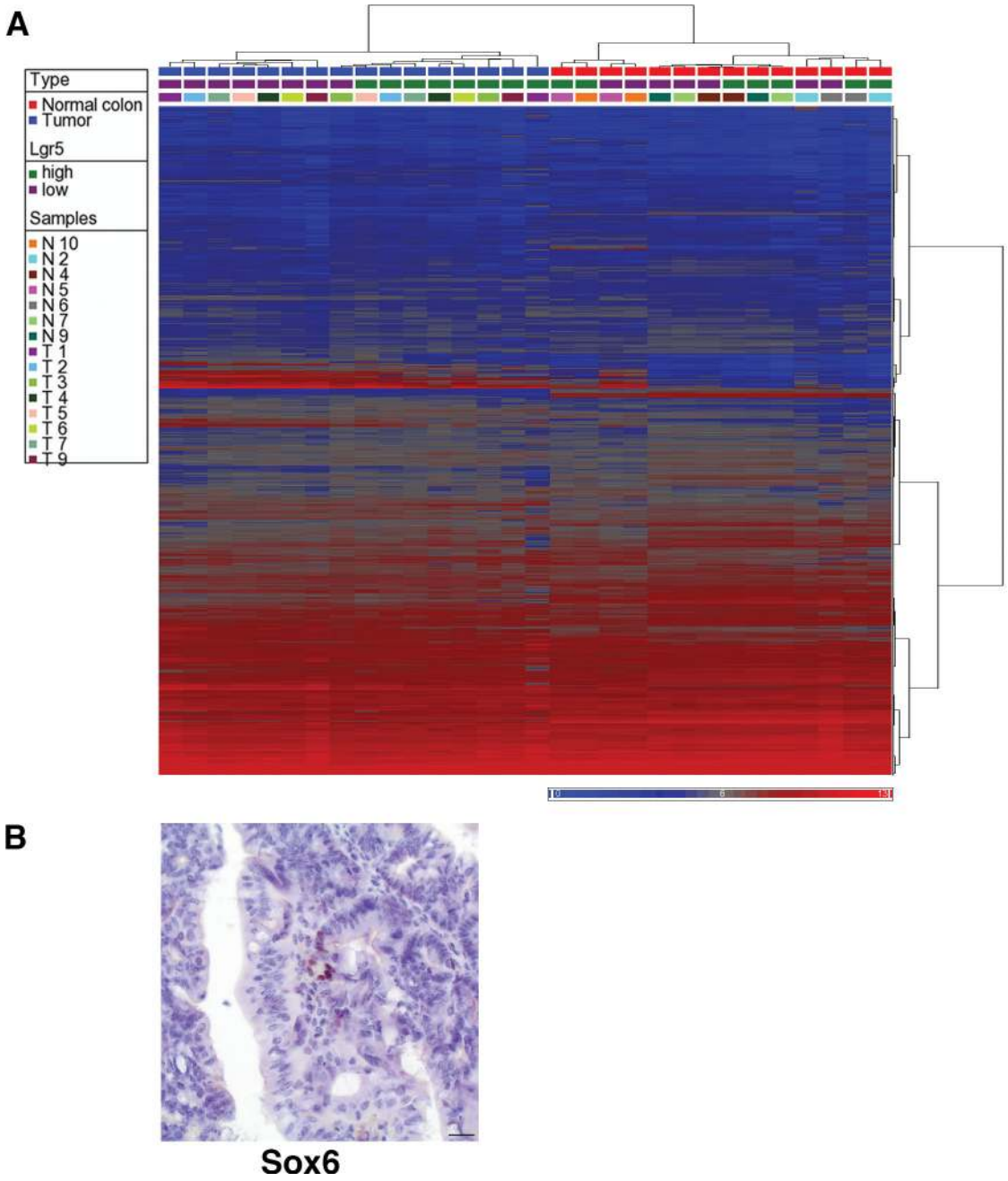

Fig. 5. Gene expression profiling of normal mouse colons and AOM/DSS-induced mouse colon tumors flow-sorted for Lgr5-EGFP. (**A**) Unsupervised hierarchical clustering based on gene expression profiles of Lgr5 high and low fractions from normal colons and AOM/DSS-induced tumors. Samples cluster by entity (normal colon or tumor) first. In tumors, the different Lgr5 fractions are clearly separated; however, in normal colons, they are separated by both Lgr5 and individual mice. (**B**) In line with our gene expression data, Sox6 expression could also be demonstrated by immunohistochemistry (positivity in a small population of scattered cells in AOM-/DSS-induced tumors). Scale bar, 20 µm.

Our functional analyses were complemented by studying global gene expression levels of cell fractions with differential *LGR5* expression. Spheres (in contrast to adherent cells) of SW480 expressed several stem cell-associated genes including *LGR5* and showed an upregulation of NOTCH signaling. Consistently, spheres appeared to be more tumorigenic than adherent cells when xenografted in nude mice. Silencing of *LGR5* resulted in the depletion of spheres. In line with our findings, *LGR5* is upregulated in spheroid cultures of colorectal CSCs and, conversely, becomes downregulated during *in vitro* differentiation of these CSCs (32). Taken together, these findings suggest that *LGR5* identifies a stem-like cell compartment in CRC, as it does in normal colorectal epithelium. This has recently been shown directly by *in vivo* lineage tracing in mouse intestinal adenomas (11).

NOTCH signaling was downregulated in SW480 CRC cells upon *LGR5* silencing, whereas genes involved in NOTCH signaling were overexpressed in *LGR5* high SW480 spheres. Consistently, *Lgr5* deficiency in the mouse during intestine development also seems to have an inhibitory effect on the Notch signaling pathway (36). In addition, downregulation of NOTCH signaling in CRC cell lines and primary CRC samples via reduction of NOTCH1 or RBPJk decreases proliferation, colony formation and tumorigenicity, whereas upregulation of NOTCH signaling via NOTCH1 results in opposite changes (3,37,38). This has also been demonstrated for other tumor entities including pancreatic, lung or breast cancer (39–41). Consistent with our gene expression analysis, it appears most likely that the reduced proliferation and migration after *LGR5*

silencing in CRC cells are a consequence of reduced NOTCH signaling (3).

Hence, our gene expression results substantiate our findings from functional assays upon *LGR5* silencing in CRC cell lines at a molecular level, suggesting LGR5 as a potential therapeutic target. For instance, Honokiol inhibits CRC growth by targeting NOTCH signaling in colorectal CSCs (42).

Pursuing stem cells as therapeutic targets might help to overcome some of the frustrations associated with current cancer treatment regimens. Cataloging gene expression data from these stem cells serves as a first step in understanding the molecular features distinguishing these cell types from the bulk of tumor cells or from normal adult tissue stem cells (43–46).

Despite the advantages of *in vitro* cultures to analyze features of stemness potential, such as ease of propagation, there are concerns that molecular changes might be induced when cells are cultured in the absence of their physiological context (13,47). Thus, we extended our gene expression profiling to *ex vivo* isolated cells. Normal mouse colons and AOM/DSS-induced mouse colon tumors from *Lgr5-EGFP* mice were flow-sorted into Lgr5 high and low epithelial cell fractions. Global gene expression analyses of flow-sorted fractions revealed an overexpression of the Wnt signaling pathway in Lgr5 high tumor cells compared with both Lgr5 low tumor cells and Lgr5 high normal cells. This supports previous findings showing that Wnt activity defines colorectal CSCs (48). Although Horst *et al.* (49) found that Wnt activity alone might not be sufficient to convey stem-like potential, our findings suggest that the combination of both Wnt signaling and Lgr5 might help to determine cells with stem-like properties in CRC.

The association of LGR5 and NOTCH signaling seen in cell lines could not be recapitulated *in vivo* when flow sorting AOM/DSS-induced mouse colon tumors for Lgr5. Also, in contrast to flow-sorted Lgr5 high and low cells from AOM/DSS-induced tumors, the Wnt signaling pathway was not significantly altered in our loss-of-function experiments in cell lines, though tending to be higher in *LGR5* high spheres compared with *LGR5* low adherent cells ($P = 0.16$). The biological difference of cell lines being cultured without their physiological context might explain these findings. Increasing evidence indicates that not only intrinsic factors but also extrinsic factors like the microenvironment can influence the CSC phenotype. For instance, Vermeulen *et al.* (48) showed in CRC that stromal myofibroblasts surrounding CSCs not only can maintain Wnt signaling activity in CSCs but also can activate Wnt signaling in more differentiated tumor cells and thereby induce the CSC phenotype. Furthermore, there is a methodological difference that might contribute to the heterogeneity of our findings in cell lines and *ex vivo* isolated tumor cells. In the *ex vivo* model, flow-sorted Lgr5 high and low cells were compared, whereas in the cell line experiment, *LGR5* was silenced actively via shRNA and compared with the original cell population. Overall, the observed heterogeneity across the different lines and models reflects one of the major problems in CSC research.

In summary, our comprehensive functional and molecular analysis of LGR5 in CRC cell lines and AOM/DSS-induced mouse colon tumors conclusively links LGR5 to stem-like cells in CRC. LGR5 did not only serve as a marker for these stem-like CRC cells but was also of functional relevance for CRC cells, thus representing a potential therapeutic target, in particular as conditional deletion of Lgr5 in mouse guts does not seem to negatively affect normal intestinal epithelium (8). To further specify the role of LGR5 in human CRC, studies of LGR5 in primary human CRC specimens will be needed in the future and, as a prerequisite, the development of a reliable LGR5 antibody.

Supplementary material

Supplementary Material and methods, Table S1 and Figures S1–S4 can be found at http://carcin.oxfordjournals.org/

Funding

Intramural Research Program, National Institutes of Health, National Cancer Institute; German Academic Exchange Service (D.H.).

Acknowledgements

The authors thank B.Chen for help with figures and IT-related support, X.Lu for help with cell culture-related experiments, M.E.Jorge (Veterinary Technician, Animal Facility, National Institutes of Health) for help with nude mouse tumor measurements, D.Despres and B.Klaunberg (Mouse Imaging Facility, National Institutes of Health) for advice and assistance with mouse colonoscopies, B.Taylor (FACS Core Laboratory, Center for Cancer Research, National Cancer Institute, National Institutes of Health) for expert technical assistance with flow sorting, K.Wolk (Immunohistochemistry Laboratory, Institute of Pathology, University Medical Center Mannheim) for help with immunohistochemical staining and C.A.Klein (Experimental Medicine and Therapy Research, University of Regensburg) for providing expert advice.

Conflict of Interest Statement: None declared.

References

1. Fearon,E.R. *et al.* (1990) A genetic model for colorectal tumorigenesis. *Cell*, **61**, 759–767.
2. Ried,T. *et al.* (1996) Comparative genomic hybridization reveals a specific pattern of chromosomal gains and losses during the genesis of colorectal tumors. *Genes Chromosomes Cancer*, **15**, 234–245.
3. Camps,J. *et al.* (2013) Genetic amplification of the NOTCH modulator LNX2 upregulates the WNT/β-catenin pathway in colorectal cancer. *Cancer Res.*, **73**, 2003–2013.
4. Clarke,M.F. *et al.* (2006) Cancer stem cells—perspectives on current status and future directions: AACR Workshop on cancer stem cells. *Cancer Res.*, **66**, 9339–9344.
5. Visvader,J.E. *et al.* (2008) Cancer stem cells in solid tumours: accumulating evidence and unresolved questions. *Nat. Rev. Cancer*, **8**, 755–768.
6. Barker,N. *et al.* (2007) Identification of stem cells in small intestine and colon by marker gene Lgr5. *Nature*, **449**, 1003–1007.
7. Carmon,K.S. *et al.* (2011) R-spondins function as ligands of the orphan receptors LGR4 and LGR5 to regulate Wnt/beta-catenin signaling. *Proc. Natl Acad. Sci. USA*, **108**, 11452–11457.
8. de Lau,W. *et al.* (2011) Lgr5 homologues associate with Wnt receptors and mediate R-spondin signalling. *Nature*, **476**, 293–297.
9. Barker,N. *et al.* (2009) Crypt stem cells as the cells-of-origin of intestinal cancer. *Nature*, **457**, 608–611.
10. Visvader,J.E. (2011) Cells of origin in cancer. *Nature*, **469**, 314–322.
11. Schepers,A.G. *et al.* (2012) Lineage tracing reveals Lgr5+ stem cell activity in mouse intestinal adenomas. *Science*, **337**, 730–735.
12. Merlos-Suárez,A. *et al.* (2011) The intestinal stem cell signature identifies colorectal cancer stem cells and predicts disease relapse. *Cell Stem Cell*, **8**, 511–524.
13. Gaiser,T. *et al.* (2011) Genome and transcriptome profiles of CD133-positive colorectal cancer cells. *Am. J. Pathol.*, **178**, 1478–1488.
14. Neufert,C. *et al.* (2007) An inducible mouse model of colon carcinogenesis for the analysis of sporadic and inflammation-driven tumor progression. *Nat. Protoc.*, **2**, 1998–2004.
15. Bongers,G. *et al.* (2010) The cytomegalovirus-encoded chemokine receptor US28 promotes intestinal neoplasia in transgenic mice. *J. Clin. Invest.*, **120**, 3969–3978.
16. Camps,J. *et al.* (2008) Chromosomal breakpoints in primary colon cancer cluster at sites of structural variants in the genome. *Cancer Res.*, **68**, 1284–1295.
17. Grade,M. *et al.* (2007) Gene expression profiling reveals a massive, aneuploidy-dependent transcriptional deregulation and distinct differences between lymph node-negative and lymph node-positive colon carcinomas. *Cancer Res.*, **67**, 41–56.
18. McClanahan,T. *et al.* (2006) Identification of overexpression of orphan G protein-coupled receptor GPR49 in human colon and ovarian primary tumors. *Cancer Biol. Ther.*, **5**, 419–426.
19. Uchida,H. *et al.* (2010) Overexpression of leucine-rich repeat-containing G protein-coupled receptor 5 in colorectal cancer. *Cancer Sci.*, **101**, 1731–1737.
20. Kai,K. *et al.* (2009) Maintenance of HCT116 colon cancer cell line conforms to a stochastic model but not a cancer stem cell model. *Cancer Sci.*, **100**, 2275–2282.

21. Yeung,T.M. *et al.* (2010) Cancer stem cells from colorectal cancer-derived cell lines. *Proc. Natl Acad. Sci. USA*, **107**, 3722–3727.
22. Kanwar,S.S. *et al.* (2010) The Wnt/beta-catenin pathway regulates growth and maintenance of colonospheres. *Mol. Cancer*, **9**, 212.
23. Huang,E.H. *et al.* (2009) Aldehyde dehydrogenase 1 is a marker for normal and malignant human colonic stem cells (SC) and tracks SC overpopulation during colon tumorigenesis. *Cancer Res*., **69**, 3382–3389.
24. Fang,X. *et al.* (2010) ChIP-seq and functional analysis of the SOX2 gene in colorectal cancers. *OMICS*, **14**, 369–384.
25. Muñoz,J. *et al.* (2012) The Lgr5 intestinal stem cell signature: robust expression of proposed quiescent '+4' cell markers. *EMBO J*., **31**, 3079–3091.
26. Ried,T. *et al.* (2012) The consequences of chromosomal aneuploidy on the transcriptome of cancer cells. *Biochim. Biophys. Acta*, **1819**, 784–793.
27. Guda,K. *et al.* (2004) Carcinogen-induced colon tumors in mice are chromosomally stable and are characterized by low-level microsatellite instability. *Oncogene*, **23**, 3813–3821.
28. Rosenberg,D.W. *et al.* (2009) Mouse models for the study of colon carcinogenesis. *Carcinogenesis*, **30**, 183–196.
29. Tanese,K. *et al.* (2008) G-protein-coupled receptor GPR49 is up-regulated in basal cell carcinoma and promotes cell proliferation and tumor formation. *Am. J. Pathol*., **173**, 835–843.
30. Walker,F. *et al.* (2011) LGR5 is a negative regulator of tumourigenicity, antagonizes Wnt signalling and regulates cell adhesion in colorectal cancer cell lines. *PLoS One*, **6**, e22733.
31. Simon,E. (2012) [Abstracts of the 96th Annual Meeting of the German Society of Pathology. May 31-June 3, 2012. Berlin, Germany]. *Pathologe*, **33** (suppl. 1), 5–175.
32. Kemper,K. *et al.* (2012) Monoclonal antibodies against Lgr5 identify human colorectal cancer stem cells. *Stem Cells*, **30**, 2378–2386.
33. Al-Kharusi,M.R. *et al.* (2013) LGR5 promotes survival in human colorectal adenoma cells and is upregulated by PGE2: implications for targeting adenoma stem cells with NSAIDs. *Carcinogenesis*, **34**, 1150–1157.
34. Nakata,S. *et al.* (2013) LGR5 is a marker of poor prognosis in glioblastoma and is required for survival of brain cancer stem-like cells. *Brain Pathol*., **23**, 60–72.
35. Kendziorra,E. *et al.* (2011) Silencing of the Wnt transcription factor TCF4 sensitizes colorectal cancer cells to (chemo-) radiotherapy. *Carcinogenesis*, **32**, 1824–1831.
36. Garcia,M.I. *et al.* (2009) LGR5 deficiency deregulates Wnt signaling and leads to precocious Paneth cell differentiation in the fetal intestine. *Dev. Biol*., **331**, 58–67.
37. Zhang,Y. *et al.* (2010) Notch1 regulates the growth of human colon cancers. *Cancer*, **116**, 5207–5218.
38. Sikandar,S.S. *et al.* (2010) NOTCH signaling is required for formation and self-renewal of tumor-initiating cells and for repression of secretory cell differentiation in colon cancer. *Cancer Res*., **70**, 1469–1478.
39. Bao,B. *et al.* (2011) Notch-1 induces epithelial-mesenchymal transition consistent with cancer stem cell phenotype in pancreatic cancer cells. *Cancer Lett*., **307**, 26–36.
40. Xie,M. *et al.* (2012) Activation of Notch-1 enhances epithelial-mesenchymal transition in gefitinib-acquired resistant lung cancer cells. *J. Cell. Biochem*., **113**, 1501–1513.
41. Simmons,M.J. *et al.* (2012) NOTCH1 inhibition *in vivo* results in mammary tumor regression and reduced mammary tumorsphere-forming activity *in vitro*. *Breast Cancer Res*., **14**, R126.
42. Ponnurangam,S. *et al.* (2012) Honokiol in combination with radiation targets notch signaling to inhibit colon cancer stem cells. *Mol. Cancer Ther*., **11**, 963–972.
43. Reya,T. *et al.* (2001) Stem cells, cancer, and cancer stem cells. *Nature*, **414**, 105–111.
44. Fabrizi,E. *et al.* (2010) Therapeutic implications of colon cancer stem cells. *World J. Gastroenterol*., **16**, 3871–3877.
45. Nguyen,L.V. *et al.* (2012) Cancer stem cells: an evolving concept. *Nat. Rev. Cancer*, **12**, 133–143.
46. Marusyk,A. *et al.* (2012) Intra-tumour heterogeneity: a looking glass for cancer? *Nat. Rev. Cancer*, **12**, 323–334.
47. Snippert,H.J. *et al.* (2011) Tracking adult stem cells. *EMBO Rep*., **12**, 113–122.
48. Vermeulen,L. *et al.* (2010) Wnt activity defines colon cancer stem cells and is regulated by the microenvironment. *Nat. Cell Biol*., **12**, 468–476.
49. Horst,D. *et al.* (2012) Differential WNT activity in colorectal cancer confers limited tumorigenic potential and is regulated by MAPK signaling. *Cancer Res*., **72**, 1547–1556.

Received August, 1, 2013; revised October 29, 2013;
accepted November 6, 2013